Received: 21 June 2017 | Revised: 27 September 2017 | Accepted: 11 October 2017

DOI: 10.1002/er.3941

RESEARCH ARTICLE

WILEY INTERNATIONAL JOURNAL OF ENERGY RESEARCH

Performance of an environmentally benign acid base flow battery at high energy density

W. J. van Egmond[1,2] | M. Saakes[2] | I. Noor[2] | S. Porada[2] | C. J. N. Buisman[1,2] | H.V.M. Hamelers[2]

[1] Department of Environmental Technology, Wageningen University, Bornse Weilanden 9, 6708 WG Wageningen, The Netherlands

[2] Wetsus, European Centre of Excellence for Sustainable Water Technology, Oostergoweg 9, 8911 MA Leeuwarden, The Netherlands

Correspondence
C. J. N. Buisman, Department of Environmental Technology, Wageningen University, Bornse Weilanden 9, 6708 WG Wageningen, The Netherlands.
Email: cees.buisman@wur.nl

Summary

An increasing fraction of energy is generated by intermittent sources such as wind and sun. A straightforward solution to keep the electricity grid reliable is the connection of large-scale electricity storage to this grid. Current battery storage technologies, while providing promising energy and power densities, suffer from a large environmental footprint, safety issues, and technological challenges. In this paper, the acid base flow battery is re-established as an environmental friendly means of storing electricity using electrolyte consisting of NaCl salt. To achieve a high specific energy, we have performed charge and discharge cycles over the entire pH range (0–14) at several current densities. We demonstrate stable performance at high energy density (2.9 Wh L^{-1}). Main energy dissipation occurs by unwanted proton and hydroxyl ion transport and leads to low coulombic efficiencies (13%–27%).

KEYWORDS

acid base flow battery, bipolar membrane, co-ion transport, energy efficiency, ion exchange membranes, renewable energy storage, sustainable materials

1 | BACKGROUND

Reliable and sustainable power supply requires large-scale electricity storage, as most renewable energy sources are intermittent in their nature.[1-4] At the same time, large-scale electricity storage based on current battery technology raises environmental concerns as their production needs scarce resources that have a high energy demand both for extraction and recycling.[5-8] On account of these disadvantages, development of a more sustainable battery is required. Such a battery is based on abundant, easily extractable, and recyclable chemicals. A few examples of recently published work on sustainable batteries include an iron redox flow battery,[9] an iron-air battery,[10] a metal free flow battery based on 9,10-anthraquinone-2,7-disulphonic acid and Br_2/Br^-,[11] and a NaCl concentration gradient flow battery (CGFB).[12,13] Although the CGFB has low environmental impact, energy density and power density are too low to be attractive for practical application. In this work, we show that the energy density and power density of the CGFB can be improved by implementing a bipolar membrane. The studied system is an energy storage system based on a reversible acid-base reaction. In this system called acid base flow battery (AB-FB), energy is being stored in acid and base solutions created by the bipolar membrane. The charge step of the AB-FB is similar to the well-known bipolar membrane electro dialysis (BPM-ED). BPM-ED converts NaCl solutions into NaOH and HCl solutions by spending electric power to separate protons and hydroxyl ions from water dissociation from the bipolar

junction inside a bipolar membrane. Energy is recovered by performing the opposite process, neutralizing the acid and base at the bipolar junction inside the bipolar membrane to form water. The process is therefore also distinctly different from the acid base electrochemical flow battery (eg, Sáez et al[14] and Ludwig[15]) which is dependent on electrode reactions involving hydrogen gas and platinum as catalyst. Potentially, the AB-FB has several environmental and safety advantages compared with typical battery or redox flow battery systems. First of all, the AB-FB system does not use any precious, toxic, or scarce materials which are, in addition to being expensive, sometimes also difficult or energy intensive to recycle.[16-18] Secondly, the solution used in an AB-FB is NaCl solution which can be derived from and recycled back to seawater which is cheap and abundantly available. In a real sized AB-FB, up to hundreds of membrane cells in series are sandwiched between 2 electrodes (Figure 1). Unlike redox flow batteries, the amount of electrodes necessary in an AB-FB is brought back to a total of 2. These electrodes do not necessarily require metals; they can be made of an environmental friendly source of carbon.[19] Additionally, an environmental friendly battery consumes little energy to be produced. A useful metric is the energy stored on invested, which relates the amount of energy a battery system stores over its entire lifetime to the energy it costs to produce the system.[20] Energy storage systems which use mostly natural materials (f.e. PHS—water or CAES—air) have the highest scores and are considered to be very environmental friendly in terms of energy consumption during production.[8,20] Because an AB-FB also uses mostly natural materials, the AB-FB has the potential to reach similar high energy stored on invested values. Next to the environmental advantages, the AB-FB largest advantage is safety. Fire or explosion hazard is negligible. Also, it is impossible that air, soil, or natural waters are damaged by leaching toxic chemicals.

An AB-FB has a theoretical energy density of 11.1 Wh L^{-3} when a maximum of 1 M of acid and base is used (as is done in this study). This study reports a measured energy density of 2.9 Wh L^{-3}. The difference between theoretical and measured capacity is mainly caused by co-ion transport as will be shown later. Yet, if co-ion transport could be minimized, the theoretical energy density of an AB-FB could be much higher because more concentrated solutions could be used (eg, ~44 Wh L^{-3} [21] for 4 M of acid and base solutions). Please note that the energy density is expressed for the volume of acid and base solutions as these are the energy carrying solutions. The salt solution does also consume space as well as the redox solution, the membrane system, housing, pumps etc., the sizes of which can fluctuate and can be freely chosen

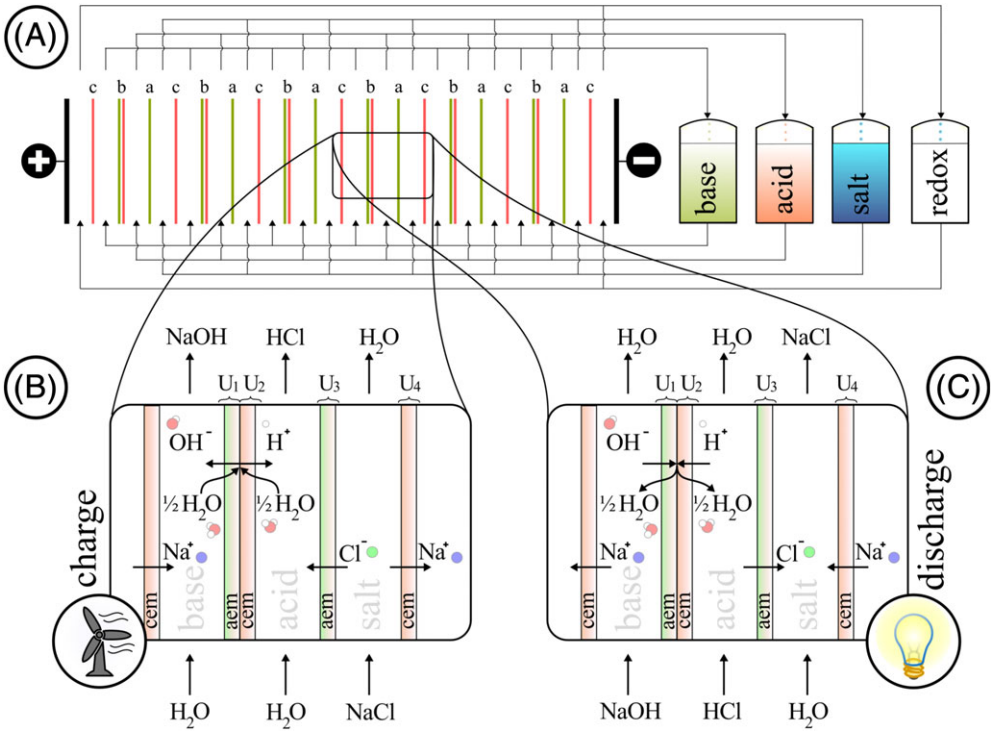

FIGURE 1 A conceptual drawing of an acid base flow battery (AB-FB). A, On the right side, the reservoirs with solutions are shown. On the left, the membrane assembly is shown. Between 2 electrodes, many membranes (up to hundreds) are stacked in a repetitive manner. B, Close-up of a single cell (bipolar membrane, consisting of anion exchange material and cation exchange material, anion exchange membrane and cation exchange membrane) with the water dissociation process and mass transport. C, Close-up of a single cell during discharge with the neutralization of the acid and base and mass transport. Please note that voltage lost at the electrodes by the redox reaction is negligible compared with the voltage generated by many membranes [Colour figure can be viewed at wileyonlinelibrary.com]

to some extent. Practical energy densities will therefore be somewhat lower as these volumes should be included. Typical redox flow batteries such as Vanadium or ZnBr redox flow batteries show energy densities in the range of 16 to 35 Wh L^{-3} and 20 to 65 Wh L^{-3},[21-23] respectively. Although the measured energy density of an AB-FB so far is a factor smaller compared with RFBs, it is already comparable to pumped hydro systems (PHS, 0.5–2 Wh L^{-3}) and compressed air systems (CAES, 2–6 Wh L^{-3}).[24] This would already make the AB-FB an option to store surplus sun and wind energy on the daily to weekly scale just as PHS and CAES are used. An AB-FB can be placed anywhere and has no geographical constraints like PHS or CAES[25] and is scalable.

Early work on the AB-FB concept was done in the 1970s by Ramp[26] where the author discussed different cell designs including the design used in this study. In this work, however, the author tested another concept using Pd electrodes and phosphoric acid without bipolar membranes. The next published study about the AB-FB concept was published by Emrén et al in the '80s.[27] They used the same stack design as used in this study but reported an extremely low energy efficiency of 0.1%. Zholkovskij et al published experimental work on another AB-FB concept in the '90s.[28] Zholkovskij et al chose to charge the battery only up to 0.03 M acid/base and to leave the acid/base solution stationary inside the membrane assembly. They reported a specific energy up to 0.1 Wh kg^{-1} (acid and base combined). In the same year, Pretz et al[29] also published a study where they use the AB-FB concept as a fuel cell. They only discharge and use pure acid and base solutions. They reported maximum discharge efficiencies with 1 M acid and base of <1%. A recent study by Kim et al[30] reports an energy density up to 0.9 Wh L^{-1} (based on unspecified volumes). Their cell design is similar to the design used in this study except for their electrodes. The cell design is based on a patent[31] where carbon electrodes are used in combination with a Fe^{2+}/Fe^{3+} redox couple to avoid gas evolving redox reactions. Their choice of Fe^{2+}/Fe^{3+} redox couple in combination with cation exchange membranes next to the electrode compartments led to iron ion migration from the electrode compartments to the base compartment. Here, the iron precipitated leading to unstable performance. In addition, they reported that the anion exchange layer of their bipolar membrane was damaged by the alkaline solution. Although the principle of the AB-FB is known, no study is known which experimentally operates the AB-FB in a stable way at sufficient energy density (using the whole pH range) with reasonable efficiency.

In this study, we provide experimental validation that it is possible to have stable operation of an AB-FB at high energy density (pH range 0–14). Low round-trip efficiency remains an issue for the AB-FB. Therefore, we study round-trip efficiency in more detail using a new set of analytical expressions to describe and quantify the energy efficiency of the AB-FB in terms of different energy dissipation sources (ohmic losses, non-ohmic losses, and co-ion losses). We show the contribution of each type of energy loss in combination with coulombic efficiency, voltage efficiency, and energy efficiency as function of current density. Also, we experimentally determined what the highest allowable discharge current density is before delamination of the bipolar membrane occurs. Finally, we discuss the optimal mode of operation and future directions to improve the round-trip efficiency.

2 | THEORY

To assess performance and power dissipation of an AB-FB, a theoretical framework is provided. The framework assumes ideal selective membranes and gives an upper limit for the specific energy. Figure 1 shows how an AB-FB works.

Figure 1A shows the 2 major components of an AB-FB, the electrode membrane assembly which is the power unit on the left and the electrolyte reservoirs where energy is stored on the right. A typical power unit is very similar to the designs of BPM-ED systems.[32-36] It consists of 2 electrodes where up to hundreds of membranes are placed in between. Three different types of membranes are present and stacked in alternate fashion: cation exchange membranes (c), bipolar membranes (b), and anion exchange membranes (a). Between the membranes, a spacer is placed which is permeable to the electrolyte solutions. The space between 2 membranes is called a compartment. Three compartments and 3 membranes (one of each type) together is called a cell. Many of these cells are thus placed in series between the electrodes. The electrolyte solutions are pumped through the compartments and recycled back to the reservoirs. The extra reservoir on the right side contains a solution which facilitates a redox reaction on the electrodes. This solution is pumped only to the 2 electrode compartments where it converts the ionic current from the membranes to an electric current at the electrodes. The redox reaction used in this study is the electrolysis reaction of water (water decomposed into O_2 and protons at the anode and into H_2 and hydroxyl ions at the cathode), but many other redox reactions are possible. Two examples of electrolyte solutions (that are in contact with the anode and cathode) are NaCl[37,38] and Na_2SO_4.[33,39] Just as in BPM-ED systems, the energy consumed by the redox reaction occurring at the electrodes is considered negligible compared with the amount of energy which is stored or extracted from the processes at the membranes. To understand how energy is stored in the AB-FB system, Figure 1B zooms

in on a single cell. The first compartment is connected to the "base" reservoir. The first membrane is a bipolar membrane. A bipolar membrane is made by fusing an anion exchange membrane (aem) and a cation exchange membrane (cem) together, typically with a catalyst in the aem and/or cem.[33,40] Anion exchange membranes are made of polymers containing fixed positive charges.[32,41] The positive fixed charges allow anions to enter the membrane but block cations and therefore make the membrane charge selective. Cation exchange membranes are identical except for the sign of the fixed charges, and thus they are selective towards cations. The second compartment is connected to the "acid" reservoir. At the start of the charge process, the flow battery is empty, and in all reservoirs only ordinary NaCl solutions are present. Once potential is applied at the electrodes, ions in solution and inside the membranes will start to move according to the electric field. Inside the bipolar membrane, initially sodium and chloride ions will move out of the membrane. As soon as these ions are depleted, water dissociation occurs inside the bipolar membrane at the interface of the aem and cem. Protons and hydroxyl ions are created by a dissociation reaction of water while interacting with weakly basic or acidic groups present at the membrane surface area.[42-44] Following Simons and Strathmann,[42-44] the following reactions can occur (Equation 1)

$$\begin{aligned} B + H_2O &\leftrightarrow BH^+ + OH^- \\ BH^+ + H_2O &\leftrightarrow B + H_3O^+ \end{aligned} \quad (1)$$

and

$$\begin{aligned} A^- + H_2O &\leftrightarrow AH + OH^- \\ AH + H_2O &\leftrightarrow A^- + H_3O^+ \end{aligned}$$

where B is a neutral base, BH^+ the catalytic active center (typically the fixed charged group on the anion exchange membrane), A^- the fixed group on the cation exchange membrane, and AH a neutral acid.[42] Different catalysts are added for promoting the water dissociation reaction.[40] Examples include carboxylic acid,[44] tertiary amines,[45] and phosphoric acid.[46]

In Figure 1B, we see that base compartment is gaining hydroxyl ions and the acid compartment is gaining protons. To account for electroneutrality in both the "acid" and "base" compartments, the extra "salt" solution compartment is added. This compartment provides sodium ions to the base solution and chloride ions to the acid solution. The extra 2 membranes are present to prevent the 3 solutions from mixing. The result of the charging process is that electric energy is spent, the acid reservoir becomes acidic, the base reservoir becomes alkaline, and the concentration of salt in the salt reservoir decreases. The final concentration of the salt reservoir in charged state depends on the choice in size of the reservoir and starting concentration. In this study, the concentration of the salt reservoir in the charged state was 0.214 M (refer to Section 3.2 for starting volume and concentration).

In the discharge process, current direction is reversed (Figure 1C). In this case, all ions move in opposite direction so that protons and hydroxyl ions recombine again inside the bipolar membrane to form water, thus neutralizing the acid and base solution. The salt compartment gains both sodium and chloride ions again, and the salt concentration returns to its original level. To understand how energy is harvested in this process, we show the membrane potentials involved. At the interface of the bipolar membrane where both ion exchange materials touch, the concentration of protons and hydroxyl ions is very low (10^{-7} M). In a charged battery, the concentration of hydroxyl ions and protons inside the base and acid solutions is much higher (1 M), and because of Donnan exclusion, a membrane potential is created over each layer of ion exchange material (Equation 2, U_1 and U_2). In a charged flow battery, the concentration of salt in the salt reservoir is low. In this study, it is 0.214 M of NaCl. Because the concentrations of chloride (1 M) in the acid reservoir and sodium (1 M) in the base reservoir are higher, also a membrane potential develops over the extra anion exchange membrane (U_3) and cation exchange membrane (U_4). In order to calculate an ideal membrane potential, we use the Nernst equation (Equation 2). Next, assuming ideal solutions, the membrane potentials of all membranes are summed to calculate the maximum cell potential (Equation 2)

$$\begin{aligned} U_1 &= \frac{RT}{zF}\ln\left(\frac{[\mathrm{OH}^-]_{bp}}{[\mathrm{OH}^-]_{base}}\right) \approx \frac{RT}{-F}\ln\left(\frac{10^{-7}}{1}\right) = 0.414 \\ U_2 &= \frac{RT}{zF}\ln\left(\frac{[\mathrm{H}^+]_{acid}}{[\mathrm{H}^+]_{bp}}\right) \approx \frac{RT}{F}\ln\left(\frac{1}{10^{-7}}\right) = 0.414 \\ U_3 &= \frac{RT}{zF}\ln\left(\frac{[\mathrm{Cl}^-]_{salt}}{[\mathrm{Cl}^-]_{acid}}\right) \approx \frac{RT}{-F}\ln\left(\frac{0.214}{1.5}\right) = 0.050 \\ U_4 &= \frac{RT}{zF}\ln\left(\frac{[\mathrm{Na}^+]_{base}}{[\mathrm{Na}^+]_{salt}}\right) \approx \frac{RT}{F}\ln\left(\frac{1.5}{0.214}\right) = 0.050 \\ \hline U_{cell} &= U_1 + U_2 + U_3 + U_4 = 0.928 \end{aligned} \quad (2)$$

where U_1 to U_4 Nernst potentials correspond to each membrane layer depicted in Figure 1C and U_{cell} is the total cell potential (V). Because in a AB-FB, many cells are stacked in series, the voltage over the electrodes can reach up to tens of volts.

An important phenomenon which can occur inside a bipolar membrane is delamination. When the discharge current density is too high, protons and hydroxyl ions recombine that fast that the produced water cannot diffuse out of the membrane fast enough. In this case, the

2 ion exchange layers can delaminate[40] in a process also known as "ballooning" of the membrane. In a AB-FB, the discharge current densities are therefore limited by delamination. In this study, we could safely operate the AB-FB up to 15 A m^{-2}. Another reason for bipolar membrane delamination is the presence of CO_2. The base solution can absorb CO_2 from the air. When the pH of the solution changes inside the bipolar membrane, gaseous CO_2 can form leading to delamination.[40]

As the flow battery is discharged and the concentrations inside the electrolyte reservoirs change, cell potential drops. With the decrease of cell potential, the remaining energy content of the solutions drops as well. For an ideal flow battery, the remaining energy content can be calculated as a function of the acid concentration according to Equation 3[47]

$$\Delta G = \int_{10^{-7}}^{[H^+]} F U_{cell} d[H^+] \tag{3}$$

where ΔG (J L^{-1}) is the total energy content, $[H^+]$ is the concentration of protons in solution (mol L^{-1}), and F is Faraday's constant (C mol^{-1}).

Figure 2 shows how energy density of such ideal flow battery behaves as function of the pH of the acid reservoir. Please note that the base concentration is identical to the acid concentration.

The total internal resistance R_i of a flow battery is given by

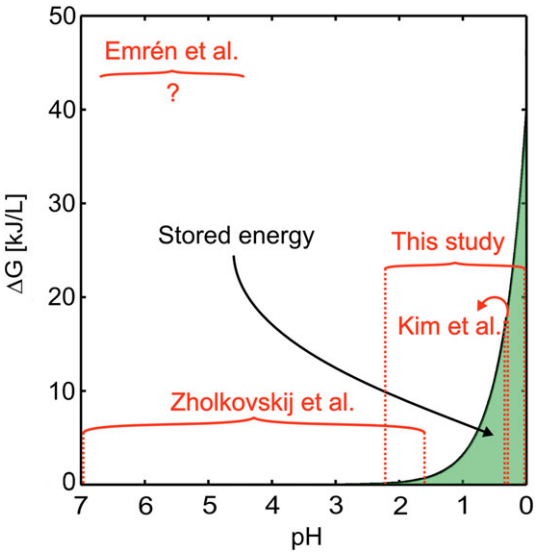

FIGURE 2 The energy content (ΔG in kJ L^{-1}) of an AB-FB as function of pH in the acid compartment. The energy content is expressed for 0.5 L acid and 0.5 L base solution and shows the maximum amount of energy which can be harvested during discharge. The operating range (in pH) for previous studies is shown as red brackets [Colour figure can be viewed at wileyonlinelibrary.com]

$$R_i = \overbrace{R_{BP} + R_{AEM} + R_{CEM} + R_{base} + R_{acid} + R_{salt} + R_{electrodes}}^{\Omega} + \overbrace{R_{non-\Omega}}^{non-\Omega} \tag{4}$$

where R_{BP} is the resistance of the bipolar membranes, R_{AEM} and R_{CEM} the resistances of the anion and cation exchange membranes, respectively, R_{base}, R_{acid}, and R_{salt} the resistances of the solutions compartments, and $R_{electrodes}$ the resistance of the rinse solution compartments plus the resistance of the extra cation exchange membrane (see Figure 2). Together, these resistances constitute the ohmic resistance (denoted as Ω in Equation 4) of the flow battery. In practice, many cells will be put in series so that $R_{electrodes}$ becomes negligible. Because of concentration polarization at the membrane interface when current is applied, non-ohmic resistance arises. This is represented in Equation 4 by $R_{non\text{-}\Omega}$.

Because of losses due to internal resistance, measured cell potential U is given by

$$U = U_{cell} - IR_i \tag{5}$$

where I is current. The round-trip efficiency, η_{RTE}, is an important figure of merit for all storage technologies. It is the ratio of energy released at discharge over energy consumed during charge. For constant current experiments, it can also be calculated by multiplying the coulombic efficiency and voltage efficiency.[12,48]

$$\eta_{RTE} = \frac{\int_0^{t_d} I_d U_d dt}{\int_0^{t_c} I_c U_c dt} = \eta_{CE}\eta_{VE} \tag{6}$$

where subscripts d and c stand for discharge and charge, respectively. Total time for charge/discharge is given by t, the applied current by I, and the measured potentials during charge and discharge are given by U. The coulombic efficiency η_{CE} is the ratio of total charge transferred during discharge over the total charge transferred during charge. Voltage efficiency is given by η_{VE} and is useful for determining the magnitude of internal losses due to internal resistance.

The total amount of energy lost is calculated by\

$$E_{lost} = \int_0^{t_c} I_c U_c dt - \int_0^{t_d} I_d U_d dt \tag{7}$$

and the total amount of energy lost on internal resistance by

$$E_{Ri} = \int_0^{t_c} R_i I_c dt + \int_0^{t_d} R_i I_d dt. \tag{8}$$

The difference between the total energy loss and the ohmic loss is the energy loss due to other processes as co-ion transport and water transport. In case of the AB-FB, it can be argued that this is mainly due to unwanted

transport of protons and hydroxyl ions.[26,27] This co-ion transport loss is then given by

$$E_{co-ion} = E_{lost} - E_{Ri}. \quad (9)$$

3 | MATERIALS AND METHOD

3.1 | Experimental setup

The experimental setup used in this work consists of a flow battery with membranes and electrodes arranged as depicted in Figure 1, and we study a single cell. The membrane/electrode assembly is pressed and is held together by 2 external acrylic plates. The membranes are separated by 500-μm spacers (SEFAR AG, Switzerland), and sealed with a silicon gasket. Four bottles containing base, acid, salt, and rinse solutions are connected with pumps, and solutions are pumped through the appropriate inlets and outlets. Following the procedure outlined by Veerman et al,[49] 2 Ag/AgCl reference electrodes (QM711X, QIS, The Netherlands) are placed in the rinse solutions close to the shielding cation exchange membrane. Two titanium mesh 1.0 electrodes coated with mixed metal oxide (iridium and ruthenium, Magneto Special Anodes B.V., The Netherlands) and reference electrodes are connected to a galvanostat (model IviumStat.XRi, Ivium Technologies, The Netherlands). Please note that although in this study Ti-mesh electrodes are used with precious metals, in a commercial AB-FB, many other (abundant) non-catalytic materials such as carbon or graphite could be used. Although non-catalytic electrode materials (no precious metals involved) would increase the overpotential of the redox reaction, this extra energy loss would be negligible compared with the amount of energy stored and released in the membranes. Another option is to use noble metal free electrode material like carbon or graphite felt in combination with a low-cost reversible redox couple based upon, eg, Fe(II) and Fe(III) with an appropriate ligand. That would result in low energy losses at the electrodes in combination with the use of a low-cost reversible electrochemical redox couple. The anion exchange membrane used (FAB-PK-130, Fumatech GmbH, Germany) is specifically selected for its high proton blocking property. The bipolar membrane is a low resistance Fumasep FBM (<3 Ω cm^2). The cation exchange membranes adjacent to the electrode compartments are Nafion N117 membranes (Dupont, USA) that are resistant against any unwanted Cl_2 that might form at the electrodes during charge or discharge. The effective area of each membrane is 0.01 m^2. The electrolyte solutions are pumped with a flow rate of 30 mL min^{-1}. Galvanic decoupling between both electrode compartments to avoid short circuit currents[50] is assured by adding additional bottles and using the droplet method. For safety, N_2 gas is pumped inside the bottles to remove the O_2 and H_2 mixture in the head space of the bottles.

3.2 | Experimental procedure

First, a test was performed to measure the open circuit voltage (OCV) of a fully charged flow battery. Fresh acid, base, salt, and rinse solutions were prepared. The acid solution consisted of 1 M HCl (Sigma Aldrich, USA) mixed with 0.5 M NaCl (ESCO, The Netherlands). The base solution consisted of 1 M NaOH (Sigma Aldrich, USA) mixed with 0.5 M NaCl. The salt solution consisted of 0.214 M NaCl, and the electrode rinse solution consisted of 0.5 M Na_2SO_4 (VWR, The Netherlands). The electrode rinse solution was selected from the study of Veerman et al[51] for its stability and non-toxicity. All electrolyte solutions are pumped through the flow battery with recycling. The measured OCV (0.83 V) represents the voltage where the flow battery is considered full (corresponding to 100% state of charge) and is used in next experiments as signal to stop charging.

Next, constant current density experiments (9 charge and 9 discharge experiments) were performed. At the start of each experimental run, 50 g of 0.5 M NaCl solution (ESCO, The Netherlands) was inserted in the acid and base bottles and 175 g of 0.5 M NaCl solution inside the salt bottle. The additional solution inside the salt bottle with respect to the acid and base bottle is there to reduce the concentration gradients of sodium chloride concentrations over the AEM and CEM once the flow battery is charged. The rinse solution bottle was filled with 5 kg of 0.5 M Na_2SO_4 solution (VWR, The Netherlands). The charge steps (3× 50, 100, and 150 A m^{-2}) are followed by discharge steps (3× 5, 10, and 15 A m^{-2}) yielding 9 datasets with full charge and discharge cycles. The discharge experiments are stopped once cell potential reaches zero volt. The x-axis in Figure 4 shows exactly how the datasets are compiled. The discharge current density was limited to a maximum value of 15 A m^{-2}, as the bipolar membrane was experimentally shown to delaminate at a current density of ~20 A m^{-2}.

During all constant current density experiments, the current is interrupted at regular intervals to measure the OCV. This OCV is a measure for state of charge of the flow battery. In addition, regular interruption of current allows for measurement of the internal resistance of the flow battery. By using chronopotentiometry,[52,53] the total internal resistance R_i is measured including its non-ohmic part ($R_{non\text{-}\Omega}$) and ohmic part (Equation 4).

Finally, the coulombic efficiency for the charge process is calculated. From our initial OCV test, we know

the theoretical capacity of a fully charged flow battery. The actual capacity during the charge steps is measured. By dividing the theoretical capacity with the measured capacity, the η_{CE} for charging is calculated.

4 | RESULTS AND DISCUSSION

In this section, we will first present charge and discharge behavior of an AB-FB and next discuss main energy dissipation mechanisms.

4.1 | Charge and discharge characteristics

This section shows and discusses typical charge and discharge characteristics of an AB-FB.

In Figure 3A, we show 3 complete charge-discharge cycles. Each cycle starts with neutral 0.5 M NaCl solutions in the acid, base, and salt reservoirs. The left area ("charge") shows the mean of 3 separate charge experiments with 100 A m^{-2}. To show the high reproducibility of the experiments, error bars showing 2 standard deviations from the mean are included. Charging was stopped when the flow battery acquired an OCV of 0.83 V, a value that corresponds to a pH of the acid compartment of 0 and the base compartment of 14 (Materials and Method). Three separate discharge steps are shown in the right area ("discharge") of Figure 3A, with current densities of 5, 10, and 15 A m^{-2}. The discharge experiments continued until discharge power reached zero. With increasing discharge current density, measured cell voltage decreased as expected from Equation 5 and expected resistance. At the end of the discharge curves, a steep decrease in potential occurred. This is explained by the depletion of acid and base, see Section 4.2 for more details about acid/base depletion. The vast majority of the energy is stored at the right-hand side of Figure 2 (pH 0–1). With a constant current density experiment, cell potential will decrease rapidly when the flow battery is nearly discharged (pH > 2) because most of the protons and hydroxyl ions are depleted from the acid and base compartment. This steep potential drop is a clear indication to stop the discharge step as only almost negligible energy is still available in the solutions.

Figure 3B shows total energy spent as function of time. Figure 3C shows total energy extracted as function of time. Because cell potentials remain nearly constant during charge and discharge (Figure 3A), the lines in Figure 3B,C are both nearly linear for the whole charge and discharge step except for the discharge step at the end. This implies that with exception of the very last end of the discharge step (marked with 2 asterisks), η_{VE} does depend little on how far the flow battery is charged and discharged.

In panels A to C in Figure 3 at regular intervals, a few data points are missing where the OCV is measured. Several single asterisks show examples of such intervals where temporarily the charge and discharge process is on hold.

4.2 | Main dissipation sources

This section discusses efficiency and main dissipation sources of the AB-FB to better understand how to improve

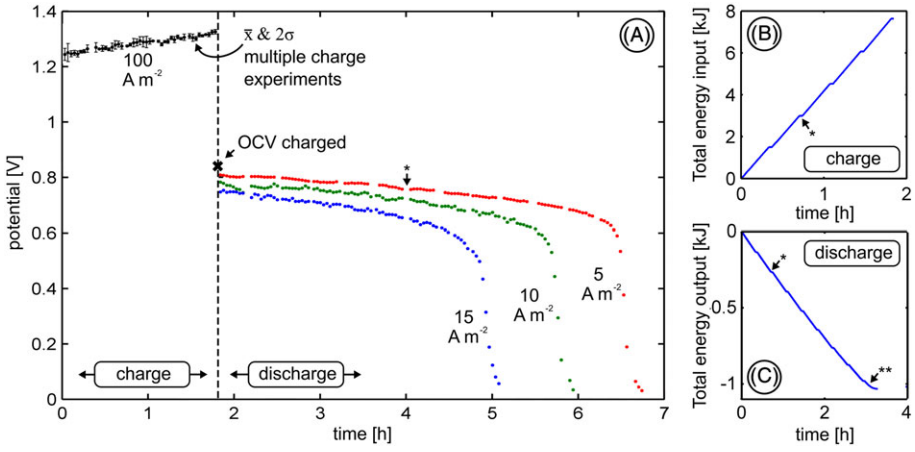

FIGURE 3 A, Charge at constant current followed by constant current discharge voltage measurements versus time in hours. At $t = 0$, the flow battery starts charging at 100 A m^{-2} until it reaches an OCV value of 0.83 V. The data points are the average values of 3 separate charge experiments repeated under identical conditions. The error bars represent 2 standard deviations (σ) from the mean. Three separate discharge current densities are shown: 5 A m^{-2} (red), 10 A m^{-2} (green) and 15 A m^{-2} (blue). B, Total energy input (kJ) in the flow battery versus time (h) during charge (100 A m^{-2}). C, Total energy output (kJ) from the flow battery versus time (h) during discharge (15 A m^{-2}). A–C, At regular intervals, current is briefly interrupted for measuring the OCV of the flow battery. The single asterisks show a few examples and explain the small areas with no voltage measurements [Colour figure can be viewed at wileyonlinelibrary.com]

its performance. Figure 4A shows various efficiencies of the AB-FB including coulombic, η_{CE}, voltage, η_{VE}, and round-trip, η_{RTE}, efficiencies of 9 charge-discharge cycles performed at different current densities. We found that the η_{CE} of all cycles is rather low and ranges between 13% and 27%.

Low η_{CE} is most likely mainly caused by unwanted mass transport.[12,26] Unwanted mass transport which occurs inside an AB-FB includes proton, hydroxyl, sodium, and chloride ions as well as water transport. The change of pH in both salt (to ~pH 2) and rinse solutions (to ~pH 2.5) indicates that leakage of protons and probably hydroxyl ions over AEM and CEM occurs. This is in line with the high mobility of these ions in aqueous environments due to their small size and the Grotthuss mechanism.[54,55] Also, the driving force for these ions is large as the concentration difference over the AEM and CEM for protons and hydroxyl ions can be as high as 1 M for a fully charged flow battery. This ion leakage leads to recombination of protons and hydroxyl ions in all compartments. Importantly, the ion recombination occurring outside the bipolar membrane does not contribute to a membrane potential, and thus substantial amount of energy is being lost inside acid-base flow battery. Ramp et al[26] and Emrén et al[27] also reported high proton and hydroxyl ion leakage as major energy dissipation source for the same system. The large energy loss by leakage of protons and hydroxyl ions is represented in Figure 4B as a green bar (39%–65%). Besides proton and hydroxyl ion leakage, also unwanted water and salt transport can take place. The acid and base carry by far most energy in the flow battery (Equation 2). Therefore, unwanted sodium and chloride ion transport is not expected to be responsible for the high energy losses presented by the green bar in Figure 4B. Also, water transport cannot account for the large energy dissipation shown by the green bar. In a CGFB, water transport causes a significant decrease in the ratio of concentrations over a membrane, leading to an appreciable loss in cell potential and energy.[12,13] In an AB-FB, however, cell potential is hardly affected by water transport, as the concentration of proton and hydroxyl ions inside the membrane remains 10^{-7} and the concentration ratio over the 2 sides of a bipolar membrane is several factors higher compared with a CGFB.

The low η_{CE} values are unacceptably low for an electricity storage system. To find out whether the charge or discharge step is responsible for the low η_{CE}, the coulombic efficiency of the charging step is calculated and shown in Table 1.

Table 1 shows increasing charge η_{CE} with increasing current density. The highest charge current density (150 A m^{-2}) even reaches a high charge η_{CE} of 88%. This can be explained by the decreasing contact times of the solutions. If the flow battery is charged fast, there is less time for the concentration gradient driven diffusion process to occur and charge η_{CE} increases. Looking at Figure 4A, we can see this is also true for discharging. With increasing discharge current, η_{CE} increases. Comparing overall η_{CE} (13%–27%) with charge η_{CE} (75%–88%), we find that the discharge step contributes most to a low overall η_{CE}. This

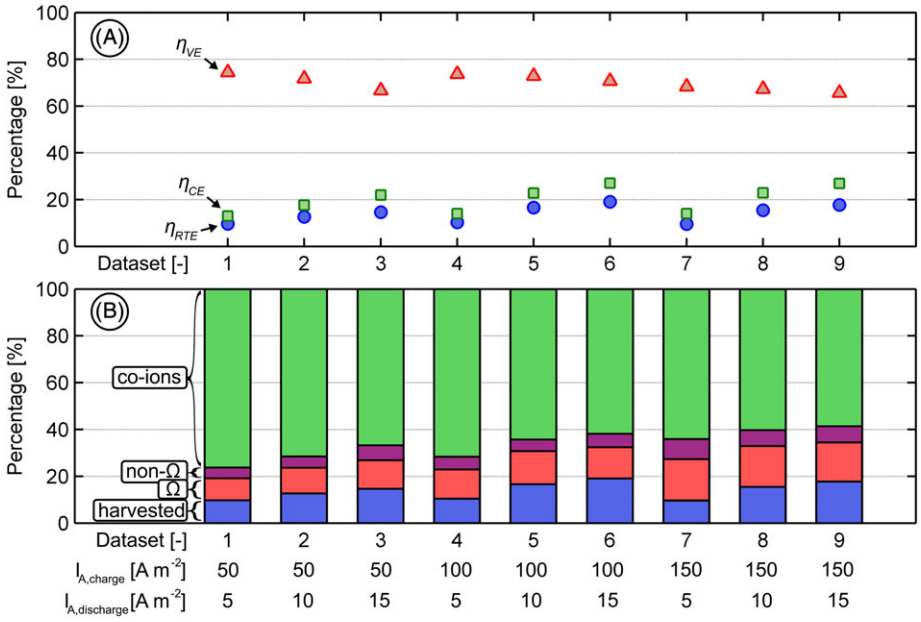

FIGURE 4 A, The voltage efficiency (η_{VE}), coulombic efficiency (η_{CE}), and round-trip efficiency (η_{RTE}) for 9 different combinations of charge currents and discharge currents. B, Distribution of energy dissipation and amount of energy harvested for 9 different combinations of charge currents and discharge currents. Each combination is called a dataset and is numbered 1 to 9. The actual charge ($I_{A,charge}$) and discharge ($I_{A,discharge}$) current densities used in each dataset are listed below panel B [Colour figure can be viewed at wileyonlinelibrary.com]

TABLE 1 Measured amount of charge in during charge phase, theoretical charge capacity, and charging η_{CE} as function of charging current density

$I_{A,c}$ (A m^{-2})	Total Charge in (Ah L^{-1})	Theoretical Charge Capacity (Ah L^{-1})	Coulombic Efficiency Charging (−)
50	35.8	26.8	0.75
100	33.3	26.8	0.80
150	30.4	26.8	0.88

is exactly what we would expect based on the longer contact times of the solutions during the discharge step. In general, we believe that the η_{CE} can be drastically improved by increasing discharge current densities. However, delamination sets an upper limit on the current density applied. Bipolar membranes with high water permeability would be necessary to allow higher discharge current densities. Another way of increasing the discharge current density without causing delamination to occur could be to include osmotic ballast in the acid and base solution to increase the rate in which water is transported out of the bipolar membrane into solution.[56]

The voltage efficiencies of all experiments, as shown in Figure 4A, are measured to be between 41% and 63%. This is lower compared with other flow batteries and CGFBs. Vanadium redox-flow batteries for example show voltage efficiencies ranging from 85% to 95%,[57] while they operate at much higher current densities of 500 to 1000 A m^{-2}. A CGFB however has a voltage efficiency ranging between 60% and 80%[12] and is most similar to the AB-FB. The measured low voltage efficiencies of an AB-FB can be explained by relatively high internal resistance. Increasing the charge current density is not favorable in terms of η_{RTE}. Comparing dataset 6 (100 A m^{-2} charge) with dataset 9 (150 A m^{-2}) for example shows that although η_{CE} is increased by increasing current density, the associated η_{VE} is much lower leading to an overall decline in η_{RTE}. A solution for increasing the η_{VE} and η_{RTE} might be using thinner solution compartments and membranes. In this case, higher charge current densities could be obtained with higher η_{VE}. Also, higher discharge current densities could be obtained because water could diffuse faster from thinner membrane layers in the bipolar membrane.

The effect of internal resistance is also visible in Figure 4B. Here, the red and purple bars show the energy losses caused by ohmic (Ω) and non-ohmic (non-Ω) resistance. The contribution of the ohmic resistance (23%–45%) is larger than the non-ohmic resistance (4%–5%). Figure 4B shows that the non-ohmic resistance increases only very little with increasing current. This can be explained by increasing concentration polarization occurring at the membrane interfaces.[58]

Round-trip efficiencies are presented in Figure 4A (as η_{RTE}) and 4B (as % energy harvested). Because of the low η_{CE} during the discharge process, the overall round-trip efficiencies are low. In summary, results show that with state-of-the art membranes, it is possible to have stable operation of the AB-FB at high energy density (pH 0–14). Round-trip efficiency is low, because of low coulombic efficiency, especially during discharge. Discharge current density is limited by delamination of the bipolar membrane. With suggested improvements, the roundtrip efficiency might be increased significantly.

5 | CONCLUSIONS

We have demonstrated that by deep charge and discharge (up to 1 M of acid and base), the AB-FB can reach power densities up to 3.7 W m^{-2} per membrane, energy densities up to 2.9 Wh kg^{-1}, and round-trip efficiencies up to 13.5%.

The measured coulombic efficiencies are moderate (13%–27%). This is mainly caused by unwanted proton transport and hydroxyl ion transport. We observed that coulombic efficiency reaches higher values at higher charge and discharge current densities. This is attributed to the shorter contact period of the solutions at high current density. The total energy lost by co-ion transport is estimated to be 39%–65%, and therefore development of proton and hydroxyl blocking membranes is timely and needed.

Reported voltage efficiencies are modest (41%–63%), and this is a result of a relatively high internal resistance caused by thick solution compartments and membranes. Key performance parameters (specific energy, power density, and round-trip efficiency) can be improved by reducing the internal resistance by using thinner solution compartments and membranes. By applying higher discharge current densities, higher power densities will be achieved. In addition, because of lower contact time of the solutions, lower proton and hydroxyl ion leakage will occur, and thus higher round-trip efficiencies would be obtained.

This work shows improved AB-FB performance and identifies routes for further improvement. In view of the potential environmental benefits of a mature AB-FB

energy storage system, further investigation of the AB-FB system as future technology for large-scale electricity storage is considered justified.

ACKNOWLEDGEMENTS

This work was performed in the cooperation framework of Wetsus, European Centre of Excellence for Sustainable Water Technology (www.wetsus.nl). Wetsus is co-funded by the Dutch Ministry of Economic Affairs and Ministry of Infrastructure and Environment, the Province of Fryslân, and the Northern Netherlands Provinces. The authors like to thank the participants of the research theme "Blue Energy" for the fruitful discussions and their financial support. In addition, the authors like to thank researchers Laura Tabernero Cogul, Eline Jagtenberg, Mei Nelissen, and Lotte van der Velde fort their efforts in performing preliminary experiments.

REFERENCES

1. Dunn B, Kamath H, Tarascon J-M. Electrical energy storage for the grid: a battery of choices. *Science (80)*. 2011;334(6058):928-935. https://doi.org/10.1126/science.1212741
2. Hirth L. The benefits of flexibility: the value of wind energy with hydropower. *Appl Energy*. 2016;181:210-223. https://doi.org/10.1016/j.apenergy.2016.07.039
3. Hameer S, van Niekerk JL. A review of large-scale electrical energy storage. *Int J Energy Res.* 2015;39(9):1179–1195. doi:https://doi.org/10.1002/er.3294.
4. Dincer I, Acar C. A review on clean energy solutions for better sustainability. *Int J Energy Res.* 2015;39(5):585-606. https://doi.org/10.1002/er.3329
5. Larcher D, Tarascon JM. Towards greener and more sustainable batteries for electrical energy storage. *Nat Chem*. 2015;7(1):19-29. https://doi.org/10.1038/nchem.2085
6. Sternberg A, Bardow A. Power-to-what?—environmental assessment of energy storage systems. *Energ Environ Sci*. 2015;8(2):389-400. https://doi.org/10.1039/C4EE03051F
7. Carbajales-Dale M, Barnhart CJ, Benson SM. Can we afford storage? A dynamic net energy analysis of renewable electricity generation supported by energy storage. *Energ Environ Sci*. 2014;7(5):1538-1544. https://doi.org/10.1039/C3EE42125B
8. Barnhart CJ, Dale M, Brandt AR, Benson SM. The energetic implications of curtailing versus storing solar- and wind-generated electricity. *Energ Environ Sci*. 2013;6(10):2804-2810. https://doi.org/10.1039/C3EE41973H
9. Tucker MC, Phillips A, Weber AZ. All-iron redox flow battery tailored for off-grid portable applications. *ChemSusChem*. 2015;8(23):3996-4004. https://doi.org/10.1002/cssc.201500845
10. McKerracher RD, Ponce de Leon C, Wills RGA, Shah AA, Walsh FC. A review of the iron–air secondary battery for energy storage. *ChemPlusChem* 2015;80(2):323–335. doi:https://doi.org/10.1002/cplu.201402238.
11. Huskinson B, Marshak MP, Suh C, et al. A metal-free organic-inorganic aqueous flow battery. *Nature*. 2014;505(7482):195-198. https://doi.org/10.1038/nature12909
12. Kingsbury RS, Chu K, Coronell O. Energy storage by reversible electrodialysis: the concentration battery. *J Memb Sci.* 2015;
13. van Egmond WJ, Saakes M, Porada S, Meuwissen T, Buisman CJN, Hamelers HVM. The concentration gradient flow battery as electricity storage system: technology potential and energy dissipation. *J Power Sources*. 2016;325:129–139. doi:https://doi.org/10.1016/j.jpowsour.2016.05.130.
14. Sáez A, Montiel V, Aldaz A. An acid-base electrochemical flow battery as energy storage system. *Int J Hydrogen Energy*. 2016;41(40):17801-17806. https://doi.org/10.1016/j.ijhydene.2016.08.141
15. Ludwig FA. Acid-base concentration cell for electric power generation. 1994;18: https://www.google.com/patents/EP0613199A1?cl=en. Accessed June 21, 2017
16. Rydh CJ. Environmental assessment of vanadium redox and lead-acid batteries for stationary energy storage. *J Power Sources*. 1999;80(1):21-29. https://doi.org/10.1016/S0378-7753(98)00249-3
17. Tarascon J-M. Towards sustainable and renewable systems for electrochemical energy storage. *ChemSusChem*. 2008;1(8–9):777-779. https://doi.org/10.1002/cssc.200800143
18. Bresser D, Paillard E, Passerini S. Chapter 6—Lithium-ion batteries (LIBs) for medium- and large-scale energy storage: current cell materials and components. *In: Advances in Batteries for Medium and Large-Scale Energy Storage*. 2015;125-211. https://doi.org/10.1016/B978-1-78242-013-2.00006-6
19. Ulaganathan M, Jain A, Aravindan V, et al. Bio-mass derived mesoporous carbon as superior electrode in all vanadium redox flow battery with multicouple reactions. *J Power Sources*. 2015;274:846-850. https://doi.org/10.1016/J.JPOWSOUR.2014.10.176
20. Barnhart CJ, Benson SM. On the importance of reducing the energetic and material demands of electrical energy storage. *Energ Environ Sci*. 2013;6(4):1083. https://doi.org/10.1039/c3ee24040a
21. Chen H, Cong TN, Yang W, Tan C, Li Y, Ding Y. Progress in electrical energy storage system: a critical review. *Prog Nat Sci*. 2009;19(3):291-312. https://doi.org/10.1016/j.pnsc.2008.07.014
22. Kear G, Shah AA, Walsh FC. Development of the all-vanadium redox flow battery for energy storage: a review of technological, financial and policy aspects. *Int J Energy Res.* 2012;36(11):1105-1120. https://doi.org/10.1002/er.1863
23. Chatzivasileiadi A, Ampatzi E, Knight I. Characteristics of electrical energy storage technologies and their applications in buildings. *Renew Sustain Energy Rev*. 2013;25(0):814-830. https://doi.org/10.1016/j.rser.2013.05.023
24. Luo X, Wang J, Dooner M, Clarke J. Overview of current development in electrical energy storage technologies and the application potential in power system operation. *Appl Energy*. 2015;137:511-536. https://doi.org/10.1016/j.apenergy.2014.09.081
25. Park J-H, Kim C-G, Lee Y-H. Efficient energy storage method by multistage pump of the energy storage system using CFD. *Int J Energy Res*. 2016;40(5):685-691. https://doi.org/10.1002/er.3432
26. Ramp FL. Secondary batteries powered by forced ionisation. *Nature*. 1979;278(5702):335-337. https://doi.org/10.1038/278335a0

27. Emrén AT, Holmström VJM. Energy storage in a fuel cell with bipolar membranes burning acid and hydroxide. *Energy*. 1983;8(4):277-282. https://doi.org/10.1016/0360-5442(83)90103-2

28. Zholkovskij EK, Müller MC, Staude E. The storage battery with bipolar membranes. *J Memb Sci*. 1998;141(2):231-243. https://doi.org/10.1016/S0376-7388(97)00306-2

29. Pretz J, Staude E. Reverse electrodialysis (RED) with bipolar membranes, an energy storage system. *Berichte der Bunsengesellschaft für Phys Chemie*. 1998;102(4):676-685. https://doi.org/10.1002/bbpc.19981020412

30. Kim J-H, Lee J-H, Maurya S, et al. Proof-of-concept experiments of an acid-base junction flow battery by reverse bipolar electrodialysis for an energy conversion system. *Electrochem Commun*. 2016;72:157-161. https://doi.org/10.1016/j.elecom.2016.09.025

31. Walther JF. Process for production of electrical energy from the neutralization of acid and base in a bipolar membrane cell. *US Pat 4311771*. 1982.

32. Strathmann H. *Ion-Exchange Membrane Separation Processes*. 9 Elsevier; 2004.

33. Wang Q, Wu B, Jiang C, Wang Y, Xu T. Improving the water dissociation efficiency in a bipolar membrane with amino-functionalized MIL-101. *J Memb Sci*. 2017;524:370-376. https://doi.org/10.1016/j.memsci.2016.11.056

34. Wilhelm FG, Pünt I, van der Vegt NFA, Strathmann H, Wessling M. Asymmetric bipolar membranes in acid-base electrodialysis. *Ind Eng Chem Res*. 2002;41(3):579-586.

35. Huang C, Xu T. Electrodialysis with bipolar membranes for sustainable development. *Environ Sci Technol*. 2006;40(17):5233-5243. https://doi.org/10.1021/es060039p

36. Xu T, Huang C. Electrodialysis-based separation technologies: a critical review. *AIChE J*. 2008;54(12):3147-3159.

37. Galama AH, Saakes M, Bruning H, Rijnaarts HHM, Post JW. Seawater predesalination with electrodialysis. *Desalination*. 2014;342:61-69. http%3A%2F%2Fwww.scopus.com%2Finward%2Frecord.url%3Feid%3D2-s2.0-84897964520%26amp%3BpartnerID%3D40%26amp%3Bmd5%3D9c7ca9177746822df0ac43c7313dc635

38. Galama AH, Daubaras G, Burheim OS, Rijnaarts H, Post JW. Seawater electrodialysis with preferential removal of divalent ions. *J Memb Sci*. 2014;452:219-228. http://edepot.wur.nl/353194

39. van Egmond WJ, Starke UK, Saakes M, Buisman CJN, Hamelers HVM. Energy efficiency of a concentration gradient flow battery at elevated temperatures. *J Power Sources*. 2017;340:71–79. https://doi.org/10.1016/j.jpowsour.2016.11.043.

40. Wilhelm FG, Vught FA. Bipolar membrane electrodialysis membrane development and transport characteristics. 2001;Dr.(ISBN 9036515270).

41. Kariduraganavar MY, Kittur AA, Kulkarni SS. Ion exchange membranes: preparation, properties, and applications. *Ion Exchange Technology I: Theory and Materials*. 2012;233-276. https://doi.org/10.1007/978-94-007-1700-8_7

42. Bazinet L. Electrodialytic phenomena and their applications in the dairy industry: a review. *Crit Rev Food Sci Nutr*. 2005;45(4):307-326. https://doi.org/10.1080/10408690490489279

43. Simons R. Strong electric field effects on proton transfer between membrane-bound amines and water [4]. *Nature*. 1979;280(5725):824-826. https://doi.org/10.1038/280824a0

44. Strathmann H, Krol JJ, Rapp HJ, Eigenberger G. Limiting current density and water dissociation in bipolar membranes. *J Memb Sci*. 1997;125(1):123-142. https://doi.org/10.1016/S0376-7388(96)00185-8

45. Zabolotskii VI, Gnusin NP, Pis'menskaya ND, Shel'deshov N V. Investigation of the catalytic activity of secondary and tertiary amino groups in the dissociation of water on a bipolar mb-2 membrane. 1986. http://www.osti.gov/scitech/servlets/purl/5365890.

46. Sheldeshov N V, Zabolotskii VI, Pis-menskaya ND, Gnusin NP. Catalysis of water dissociation by the phosphoric-acid groups of an MB-3 bipolar membrane. 1986. http://www.osti.gov/scitech/servlets/purl/6565200.

47. Wang W, Wei X, Choi D, Lu X, Yang G, Sun C. Chapter 1—Electrochemical cells for medium- and large-scale energy storage: fundamentals A2—Menictas, Chris. In: Skyllas-Kazacos M, Lim TM, eds. *Advances in Batteries for Medium and Large-Scale Energy Storage*. Woodhead Publishing; 2015:3-28 https://doi.org/10.1016/B978-1-78242-013-2.00001-7.

48. Lu R, Yang A, Xue Y, Xu L, Zhu C. Analysis of the key factors affecting the energy efficiency of batteries in electric vehicle. In: EVS 2010 - Sustainable Mobility Revolution: 25th World Battery, Hybrid and Fuel Cell Electric Vehicle Symposium and Exhibition. 2010. https%3A%2F%2Fwww.scopus.com%2Finward%2Frecord.uri%3Feid%3D2-s2.0-84907402237%26amp%3BpartnerID%3D40%26amp%3Bmd5%3Dc868dfc40e5e70cd3d15ffd75343eeba%0A.

49. Veerman J, De Jong RM, Saakes M, Metz SJ, Harmsen GJ. Reverse electrodialysis: comparison of six commercial membrane pairs on the thermodynamic efficiency and power density. *J Memb Sci*. 2009;343(1):7-15.

50. Veerman J, Post JW, Saakes M, Metz SJ, Harmsen GJ. Reducing power losses caused by ionic shortcut currents in reverse electrodialysis stacks by a validated model. *J Memb Sci*. 2008;310(1–2):418-430. https://doi.org/10.1016/j.memsci.2007.11.032

51. Veerman J, Saakes M, Metz SJ, Harmsen GJ. Reverse electrodialysis: evaluation of suitable electrode systems. *J Appl Electrochem*. 2010;40(8):1461-1474. https://doi.org/10.1007/s10800-010-0124-8

52. Vermaas DA, Saakes M, Nijmeijer K. Early detection of preferential channeling in reverse electrodialysis. *Electrochim Acta*. 2014;117:9-17. https://doi.org/10.1016/j.electacta.2013.11.094

53. Sistat P, Pourcelly G. Chronopotentiometric response of an ion-exchange membrane in the underlimiting current-range. Transport phenomena within the diffusion layers. *J Memb Sci*. 1997;123(1):121-131. https://doi.org/10.1016/S0376-7388(96)00210-4

54. Tuckerman ME, Marx D, Parrinello M. The nature and transport mechanism of hydrated hydroxide ions in aqueous solution. *Nature*. 2002;417(6892):925-929. https://doi.org/10.1038/nature00797

55. Robinson RA, Stokes RH. *Electrolyte Solutions*. Courier Corporation; 2002.

56. Kingsbury RS, Coronell O. Osmotic ballasts enhance faradaic efficiency in closed-loop. *Membrane-Based Energy Systems Environ Sci Technol*. 2016. https://doi.org/10.1021/acs.est.6b03720
57. Skyllas-Kazacos M, Kazacos G, Poon G, Verseema H. Recent advances with UNSW vanadium-based redox flow batteries. *Int J Energy Res*. 2010;34(2):182-189. https://doi.org/10.1002/er.1658
58. Vermaas DA, Saakes M, Nijmeijer K. Enhanced mixing in the diffusive boundary layer for energy generation in reverse electrodialysis. *J Memb Sci*. 2014;453(0):312-319. https://doi.org/10.1016/j.memsci.2013.11.005

How to cite this article: van Egmond WJ, Saakes M, Noor I, Porada S, Buisman CJN, Hamelers HVM. Performance of an environmentally benign acid base flow battery at high energy density. *Int J Energy Res*. 2018;42:1524–1535. https://doi.org/10.1002/er.3941